

Research Article

Effect of Rare Earth Addition on Wear Properties of Aluminum Alloy- Rice Husk Ash/Yttrium Oxide Hybrid Composites

Ahmed Moosa[†] and Abbas Yass Awad[†]

[†]Department of Materials Engineering Technology, Engineering Technical College– Baghdad, Middle Technical University, Baghdad, Iraq

Accepted 15 May 2016, Available online 18 May 2016, Vol.6, No.3 (June 2016)

Abstract

The present study deals with the wear behavior of Al-Re alloy/ RHA-Y2O3 hybrid composites. The Aluminum-Rare earth alloy (Al-Re) was used as a matrix to be reinforced with rice husk ash (RHA) and yttrium oxide (Y2O3). The Aluminum-Rare earth matrix alloy (Al-Re alloy) was prepared by melting 4032Al alloy with a standard Mg-Re alloy (AE42 alloy contains cerium and lanthanum). The desired Al-Re alloy/ RHA-Y2O3 hybrid composites were produced by using two-steps stir casting process by adding RHA: Y2O3 in weight ratios 4:0, 3:1, 2:2, 1:3 and 0:4 to Al-Re alloy such that the total reinforcement is 10wt%. Dry sliding wear, coefficient of friction, hardness, apparent density, percentage of porosity were examined. The prepared hybrid composites were characterized using optical micrograph, SEM and X-ray diffraction. The addition of rare earth element (cerium and lanthanum) increases the hardness and the density and lowers the wear rate by decreasing the porosity in the matrix, refinement of the grains and the formation of intermetallic compounds such as Al3Ce, Al4Ce and La3Al11 in matrix. In general, the wear rates of the composites are lower than alloys especially at 20N. Coefficient of friction varies inversely with increasing both applied load and volume fraction of RHA. The Al-Re alloy-Y2O3 composites have minimum wear rate. Al-Re alloy-(RHA-Y2O3)[3:1] hybrid composites have lower porosity with more grains refinement.

Keywords: Aluminum, Rice Husk Ash, Yttrium oxide, Hybrid Metal Matrix Composites, Stir casting, Wear rate, Rare earth

1. Introduction

Aluminum metal matrix composites (AMC) are far much superior to aluminum alloys due to enhanced properties and ability to possess functional properties by variety of reinforcements. The acceptability of various ceramic reinforcements further enhances the domain of AMC composites which can be used in variety of applications (Sharma *et al.*, 2015). Hybrid composites are relatively new and obtained by using two or more different kinds of reinforcement materials in a common matrix. These hybrid composites have better all around combination of properties than composites containing only a single reinforcement phase (Rajuet *et al.*, 2014). There is a demand for the use of synthetic/agro waste reinforcements to producing low cost aluminum hybrid composites. Considerable efforts have been made to use ashes produced from controlled burning of agro-wastes (Malequeet *al.*, 2012). These agro waste products such as baggase, rice husk, bamboo leaves, groundnut, and others after harvesting are usually discarded in the environment after harvesting. This is because of poor recycling technologies and awareness leading to diverse environmental challenges (Madaksonet *al.*, 2012).

One of the large agricultural wastes is rice husks generated as by-product of rice milling process. Rice husk (RH) is the outer covering of the grain of rice plant with a high concentration of silica, generally more than 80-85%. Rice husk is produced in millions of tons per year as a waste material in agricultural and industrial processes. It can contribute about 20% of its weight to rice husk ash (RHA) (Usmanet *al.*, 2014).

Stir casting is popular method in which the solid particles are imparted into the molten material and then stirred overall to get homogeneous mixture with the matrix metal (Saravananet *al.*, 2015). The advantages of this process lie in its minimum final cost of product, flexibility, simplicity and applicability to production in large quantity. The preparing composite materials by using this casting process reducing the cost about one-third to half that of another techniques (Mathur and Barnawal, 2013).

(Shridharaet *al.*, 2015) used stir casting to prepare Al-4.5% Cu alloy as the matrix with bamboo leaf ash and graphite as the filler materials. The results showed that hardness, tensile strength, and wear resistance increased with increasing the bamboo leaf ash and graphite content. Tensile strength of prepared composites is higher up to 4% BLA-6wt% graphite

*Corresponding author: Ahmed Moosa

and after this slowly decreases but higher than compared to base matrix.

Double stir casting process was used (Prasad et al., 2014) to prepare aluminum composite reinforced with various fractions of 2, 4, 6, and 8 wt.% RHA/ SiC particulates in equal proportions. It was observed that the hardness and porosity of the hybrid composite increased with increasing reinforcement wt % but the density decreased with increasing particle content. The UTS and yield strength increase with an increase in the wt% of the reinforcement particles, whereas elongation decreases with the increase in wt% reinforcement. (Usman et al., 2014) used stir casting process to prepare Al-alloy / rice husk ash composites. The results showed the ultimate tensile strength (UTS) varies from 164.374 MN/m² at 0% RHA to maximum value of 176.837 MN/m² at 10% RHA. Incorporating rice husk ash into the aluminum alloy improves its mechanical properties together with its density.

A356.4/ RHA-SiC hybrid composites with particulates up to 8% (in equal proportions) were fabricated by vortex method exhibits higher wear resistance than the unreinforced alloy (Prasad and Shoba, 2014). The increase in wear resistance can be attributed to the strengthening mechanism of the matrix which results from the thermal mismatch between the A356.4 alloy matrix and the RHA-SiC reinforcements.

The mechanical behavior of Al-Mg-Si alloy/ RHA-SiC hybrid composites was studied by (Alaneme and Adewale, 2013) used different RHA: SiC weight ratios (0:1, 1:3, 1:1, 3:1, and 1:0 to have 5, 7.5 and 10 wt% of RHA-SiC reinforcement) and two-steps stir casting method. The results showed that the composites have good casting quality with porosity less than 2.5 %. The tensile, yield, and specific strength for all composites decrease with increase in the weight proportion of RHA in the RHA-SiC reinforcement.

The addition of 3, 6, 9 and 12 wt% RHA to AlSi10Mg alloy matrix will increase ultimate tensile strength, compressive strength and hardness of the composite as reported by Saravanan and Kumar, (2013). The ductility decreases with increase in the weight fraction of RHA. However, for composites with more than 12% weight fraction of RHA particles, the tensile strength was decreased.

(Mittal and Muni, 2013) studied the mechanical properties of Al 6061 alloy/RHA- Cu hybrid metal matrix composites using stir casting techniques. The rice husk ash was added in 8, 16, 24, 32 wt% and copper 3 wt% to the molten metal. It was observed that specimens containing copper showed improvement in the hardness than specimens containing only rice husk ash. The hardness increased linearly with increasing the weight percentage of reinforcing particles.

(Alaneme and Olubambi, 2013) prepared Al-Mg-Si alloy / RHA-Al₂O₃ hybrid composite with 2, 3, and 4 wt % RHA and the total reinforcement is 10 wt % using double stir casting process. They found that the coefficient of friction and the wear rate of the composites increase with increase in RHA wt %.

The dry sliding wear behavior of Al /rice husk ash composites prepared by stir casting process was studied by (Pydi et al., 2012) using normal loads of 10N, 20N, 30N, 40N, and 50N at room temperature. The results showed that the Al /rice husk ash composite has higher wear resistance as compared to that of unreinforced aluminum. At 8 wt % RHA reinforcement, the friction coefficient increases at higher loads of 39.22N and 49.03N. This is caused by poor interfacial bonding between the reinforcement and the matrix which cause particle transferring from the matrix to the steel disc interface.

(Saleh, 2010) studied the mechanical properties of the Al-12% Si alloy modified by 0.3wt% antimony powder and reinforced with 3, 6, 9 and 12 wt% Y₂O₃ using vortex technique. The results showed that the addition of antimony leads to the microstructure refinement and change the silicon shape from the flake-like or lamellar-like to fibrous-like. The addition of Y₂O₃ particles increases the hardness and decrease the wear rate.

(Bouaeshi and Li, 2007) prepared Al/ Y₂O₃ composite and studied the effects of Y₂O₃ on microstructure, mechanical properties, and resistance to corrosive wear of aluminum composites. The results showed that microstructure of Al/ Y₂O₃ composite become finer with the increase in yttria content. However, the added yttria particles are not observed in the modified aluminum. Instead, a new phase, Al₃Y, is formed. The hardness, strength and wear rate are improved by adding Y₂O₃ and this may be due to formation of Al₃Y.

The present work is aimed to investigate the influence of the different weight ratios of rice husk ash and yttrium oxide reinforcements on the mechanical behavior Aluminum-Rare earth matrix hybrid composites.

Very limited number of literatures available on the RHA/Y₂O₃ weight ratios effect on some mechanical properties of the hybrid composites. Thus, it is important to study the effect of RHA/Y₂O₃ addition to Al-matrix alloy. Also the aim of this work is to study the effect of rare earth elements (cerium and Lanthanum) addition to aluminum alloy on wear properties of Al-Re alloy/ RHA-Y₂O₃ hybrid composites. Dry sliding wear, coefficient of friction, hardness, apparent density, percentage of porosity were examined. The prepared hybrid composites were characterized using optical micrograph, SEM and X-ray diffraction.

2. Materials and Methods

2.1 Materials

The aluminum alloy used is 4032Al-alloy (ASM, 1992) as the source for Al matrix alloy with chemical composition shown in Table 1. (Moosa & Awad 2016). The 4032Al-alloy was prepared from used Mini bus used piston.

Table 1 Chemical Composition of Al-Alloy KIA Mini Bus Piston

	Si	Cu	Mg	Fe	Ni	Zn	Cr	Al
Stand. Alloy	11-13.5	0.5-1.3	0.8-1.3	1.0 max	0.5-1.3	0.25 max	0.1 max	Bal.
Actual Alloy	12.5	1.19	0.8	0.5	0.5	0.08	0.01	Bal.

The magnesium-rare earth alloy (Mg-Re alloy) is a master alloy AE42 (Shanghai Ruizheng Chemical Technology Co., Ltd.China) with chemical analysis shown in Table 2 . The Mg-Re master alloy will be added to Al-alloy to produce Al-rare earth alloy matrix (Al-Re alloy) . The Mg- Re master alloy contains 1.2 % Ce and 0.6 % La as rare earth elements.

The yttrium oxide (Y2O3) powder with purity 99.95%, particle size less than 53 micron (Fixanal company, Germany) was used as a hybrid reinforcement filler with RHA in Al-alloy matrix composite

Table 2 Chemical Composition of AE42 Alloy

Element	Wt%
Al	3.9
Ce	1.2
La	0.6
Nd	0.4
Mn	0.3
Th	0.2
Pr	0.1
Si	0.01
Zn	<0.01
Mg	Bal

2.2 Preparation of Rice Husk Ash

The rice husk was obtained from local Iraqi mill was first washed and then sun dried for 24 hrs. The rice husk was then burned at 700 °C and left burning for 3hrs after that it was left for 12 hrs to cool down. The ash was then milled and sieved to 125 micron and then heat treated in an electrical box furnace (Carbolite, England)at a rate of 7°C/ min until the temperature is 1100 °C for 2 hours to remove carbonaceous materials and then furnace cool. The rice husk ash has black color at 700°C, while the heat treated rice husk ash has a grayish white color after heat treatment at 1100 °C as shown in Figure 1. The ash was then collected for XRF and XRD analysis.

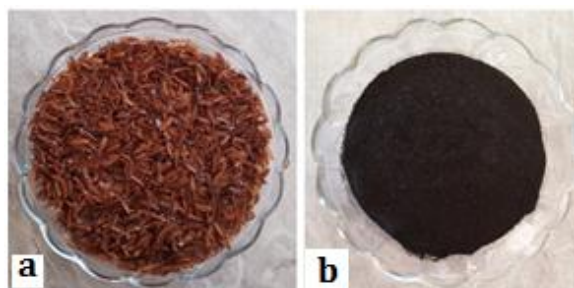


Figure 1 (a) Rice Husk (RH); (b) RHA burned at 700 °C; (c) RHA heat treated at 1100 °C for 2 hrs

2.3 Production of Al-Re Alloy / RHA-Y2O3 Hybrid Composite Preparation

The Al-Re alloy /RHA-Y2O3 hybrid composite were prepared by stir casting. The total weight of each Al-Re Alloy / RHA-Y2O3 composite is 500 gm. Each 500 gm composite casting contains 439 gm of aluminum 4032 alloy, 11 gm Mg-Re master alloy and 50 gm (RHA-Y2O3) powder with different ratios as shown in Table 3. The aluminum 4032 alloy was melted first in alumina crucible using gas fired furnace at temperature of 750 °C and kept at this temperature for 30 minutes to allow complete melting of the alloy. Then 11 gm Mg-Re alloy was added to the melt. The Y2O3 and RHA were preheated to 350 °C to remove the moisture and enhance the stacking with molten metal and then were added to the molten Al -Re alloy. The details of the addition of RHA-Y2O3 powder to the molten Al -Re alloy was reported by (Alaneme andAdewale, 2013) and our previous work (Moosa&Awad 2016). The produced Al-Re Alloy / RHA-Y2O3 hybrid composites ingot was cooled to room temperature and was then cut into samples using lathe machine for hardness, microstructure and wear test.

Table 3 Al -Rare Earth Alloy/(RHA - Y2O3)Hybrid Composites

Sample Number	Composition
Sample 1	Al-Re Alloy
Al-Re Alloy + RHA / Y ₂ O ₃	
Sample 2	Al-Re Alloy + 10% RHA + 0% Y2O3
Sample 3	Al-Re Alloy + 7.5% RHA + 2.5% Y2O3
Sample 4	Al-Re Alloy + 5% RHA + 5% Y2O3
Sample 5	Al-Re Alloy + 2.5% RHA + 7.5% Y2O3
Sample 6	Al-Re Alloy + 0% RHA + 10% Y2O3

2.4 Hardness Test

The hardness of Al-Re alloy/RHA- Y2O3 hybrid composites test samples were prepared according to ASTM E384 standard (ASM, 2000) .Hardness tests were performed using micro-Vickers hardness machine (Model: HVS-1000, USA manufacture) with a load 490 gm for 20 seconds and the average of 5

hardness readings were taken for each sample and the micro-Vickers hardness was calculated according to (ASM, 2000) :

$$HV = \frac{2000P \sin(\alpha/2)}{d^2} = 1854.4 \frac{P}{d^2} \quad (1)$$

2.5 Wear and Coefficient of Friction Measurement

Wear tests specimens were prepared according to ASTM G99-95 standard (ASM, 2000). A pin-on-disc wear test apparatus (Model: ED-201, India manufacture) was used to measure the wear rate for Al-Re alloy / (RHA- Y2O3) composites . The tests were conducted for 15 minutes at different loads: 5, 10, 15 and 20 N at room temperature using sliding speed 480 rpm using steel disc (62 HRC) and 60mm track diameter. The difference in weight before and after is the weight loss due to wear test. The wear rates determined by using the weight loss method according to the following equation(Prasad *et al.*, 2013):

$$WR = \Delta m / 2\pi r n t \quad (2)$$

Where :-

WR :- Wear rate (gm/cm)

Δm :- Weight lost (gm) which is the difference in mass of the specimens before and after every test.

t = Sliding time (minutes)

r = The radius of the specimen to the center of the disc (cm)

n = Disk speed in rpm

2.6 Apparent Density and Porosity Measurements

The apparent density and porosity were calculated according to Archimedes principle under ASTM C373-88 . The weight of the specimen was measured using digital balance type Sartorius (model: BL 210 S, Germany manufacture) with accuracy of ± 0.1 mg. The apparent density can be determined experimentally using Archimedes principle (Boopathiet *al.*, 2013) :

$$\rho_a = \left[\frac{W_a}{W_a - W_w} \right] \times \rho_w \quad (3)$$

Where

W_a = Weight of specimen in air (gm)

W_w = Weight of specimen in water (gm)

ρ_a = Apparent density of composite (gm/cm³)

ρ_w = Density of water (gm/cm³)

In general, porosity in a composite decreases the mechanical properties and decreases the corrosion resistant of the casting, therefore, the level of porosity must be kept to a minimum. However, porosity cannot be fully removed from the composite during casting process, but it can be controlled (Hashimet *al.*, 1999). The porosity percentage of the composites can be calculated as (Alaneme, 2013):

$$\% \text{ Porosity} = \frac{\rho_{th} - \rho_{ex}}{\rho_{th}} \times 100\% \quad (4)$$

Where,
 ρ_{th} the theoretical and experimental density (gm/cm³) respectively .

2.7 Microstructural Examination

The microstructure of the Al-Re alloy / (RHA- Y2O3) hybrid composites were examined using optical microscope (model: MT 71000, Meiji techno co. Ltd., Japan manufacture) with a digital camera (canon, Japan). The specimens were ground ,polished and then washed with alcohol, dried and etched using Keller's reagent (95 ml water, 2.5 ml HNO₃, 1.5 ml HCl, 1.0 ml HF) for 15 minutes (Alanemeet *al.*, 2015). Scanning electron microscope (SEM) (model: Viga-3, Belgium) was used to characterize the morphologies of the samples.

2.8 X-Ray Florescence and XRD

X-ray florescence type Spectro / Ametek, (model: XEPOS, Germany manufacture) was used to determine the elements and oxides amount in the RHA. For X-ray diffraction , the diffractometer type Shimadzu (model: XRD-6000,Japan) was used. Eight samples were tested, seven samples was cylindrical shape with 10mm diameter and 10mm height for composite and one asash. The diffractometer use Cu target is operating at 40 Kv and 30 mA. The diffractometer angle ranged depend on the type of material tested with standard wave length 1.54060 Å. The scanning process is done with speed of 5°/min. The diffraction angle ranged from 10° to 80°.

3. Results and Discussion

3.1 Rice Husk Ash Characterization

Rice husk ash was heat treatment at 1100 °C for 2 hrs. The X-ray florescence (XRF) of the heat treated rice husk ash is shown in Figure 2. The chemical composition of RHA is shown in Table 4(Moosa&Awad 2016). The RHA contains 91% silica along with 4.7 % of carbon, CaO, Fe₂O₃, Na₂O, MgO, K₂O. X-ray diffraction of treated rice husk ash was performed by scanning the ash sample between 2 θ ranging from 10° - 80° to examine the silica phases in the ash as shown in Figure 3 (Moosa & Awad 2016) . Only silica and carbon peaks were observed in the X-ray diffraction patterns. Silica phases are cristobalite and tridymite . Silica initially exists in the amorphous form in the rice husk but after heat treatment of the rice husk ash at 1100 °C for 2 hrs , the porous and amorphous phase will change to crystalline with prolonged heating process or at high temperature under oxidizing conditions. The specific surface area of the RHA is affected by combustion environment, temperature and time. This is in agreement with work of Ramezani pouret *al.*, (2009). Rice husk ash begins to transform from purely amorphous to crystalline at temperature above 500 °C. (Onojahet *al.*, 2013).

3.2 Microstructure of Al-Re Alloy

The microstructure of Al-Re alloy is shown in Figure 4 with Al-Ce phase, dendrite arm and eutectic phase. The effect of rare earth addition to Al-alloy resulted in grain refinement and dendrite arms compared with Al-master alloy. Rare earth elements make some changes in the eutectic silicon appearance, where the structure transforms from coarse plate-like silicon structure to fine fibrous eutectic morphology throughout the entire sample. Solid solubility of Ce in aluminum is about 0.05% at 636.85 °C, this solubility decreased when Si and Mg presence in aluminum alloy. Addition of Ce element to aluminum leads to precipitation of intermetallic compound, which has needle like structure (Nogitaet *al.*, 2004) and (Anasyidaet *al.*, 2010).

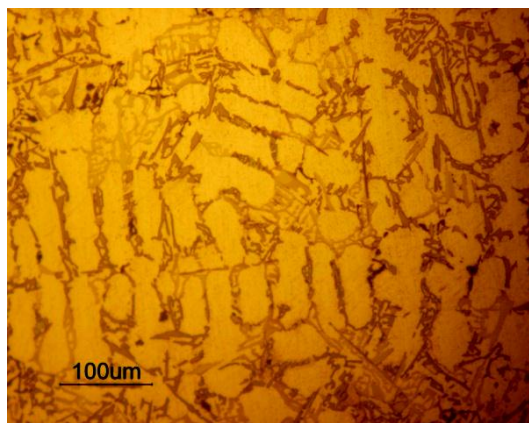


Figure 4 Microstructure of Al-Re Alloy

Table 4 Chemical composition of RHA

Elements	Wt%
SiO ₂	91
C	4.7
CaO	2.54
Fe ₂ O ₃	0.65
Na ₂ O	0.58
MgO	0.25
K ₂ O	0.123
MnO	0.035
TiO ₂	0.026
Al ₂ O ₃	0.023
others	0.031

3.3 Microstructure of Al-Re Alloy Hybrid Composites

The microstructure of Al-Re alloy-RHA composite is shown in Figure 5 with fine grains. The refinements is caused by the addition of rare earth elements to matrix alloy. The RHA is uniformly distributed with less agglomeration due to refinements of dendrites. Al-Ce intermetallic compounds are shown as needles in the matrix alloy.

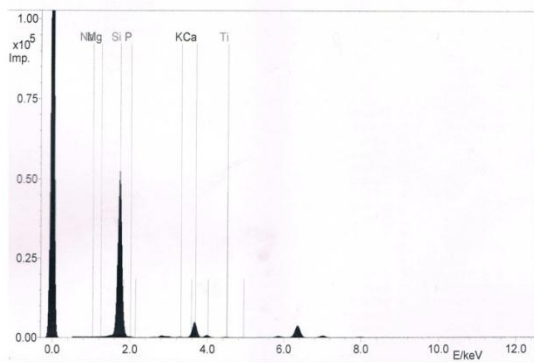


Figure 2 XRF of Rice Husk Ash at 1100 °C and 2hrs

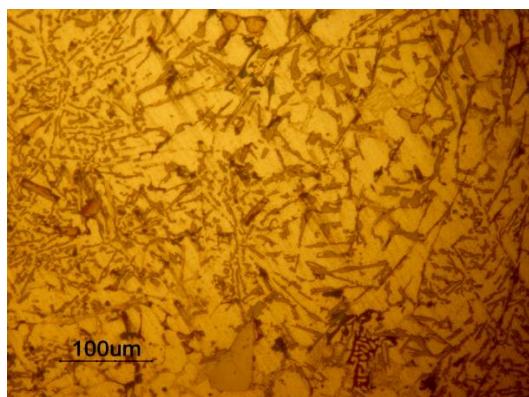


Figure 5 Microstructure of Al-Re Alloy-RHA Composite

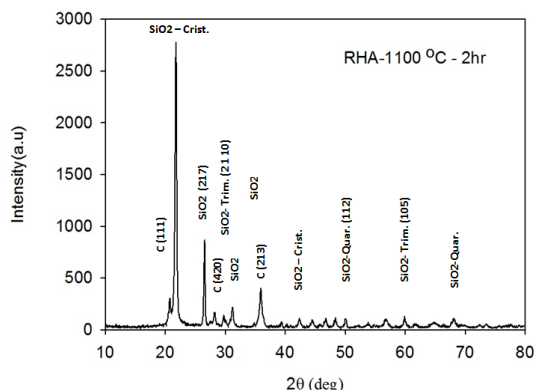


Figure 3 XRD of Heat Treated RHA

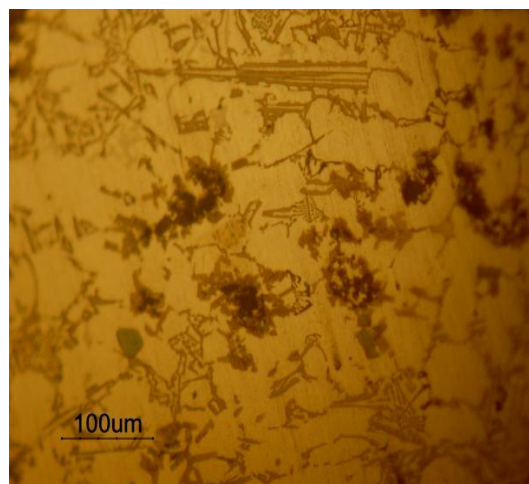


Figure 6 Microstructure of Al-Re Alloy-Y₂O₃ Composite

The microstructure of Al-Re alloy-Y2O3 composite is shown in Figure 6 with Al-Ce , Y2O3 and fine dendrites arm which are closer to each other. This fine and close dendrites can be explained by two reasons, firstly the rare earth element cause grain refinement of matrix alloy, and secondly the Y2O3 particles make refinement by increasing the nucleation site during solidification refinement by increasing the nucleation site during solidification.

The microstructure of Al-Re alloy-(RHA-Y2O3)[2:2] hybrid composite is shown in Figure 7 with Al-Ce , RHA,Y2O3 in addition to fine and closer dendrites arm to each other. The distribution of RHA and Y2O3 is more uniform with less clusters.

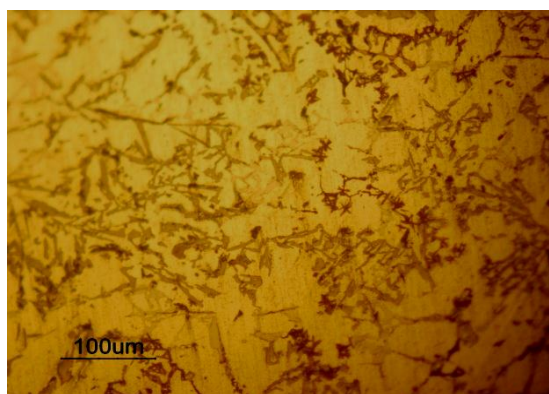
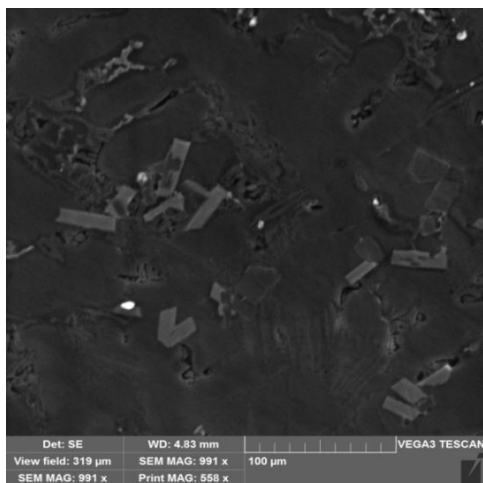


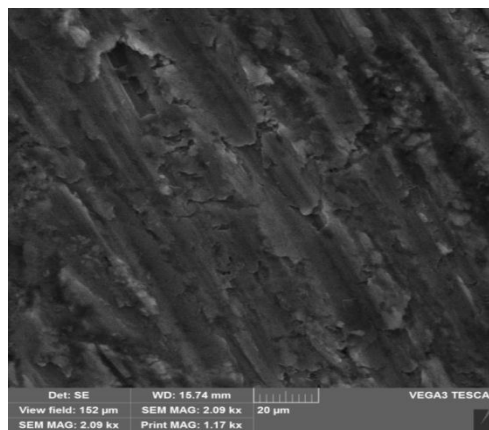
Figure 7 Microstructure of Al-Re Alloy-(RHA-Y2O3)[2:2] Hybrid Composite

3.4 SEM of Hybrid Composites

Figures 8 show SEM micrographs of Al-Re alloy-Y2O3 and Al-Re alloy-(RHA-Y2O3)[2:2] composite. A uniform distribution of the reinforcement's particles without discontinuities can be observed from these micrographs along with good bonding between matrix material and the reinforcements. The SEM micrographs showed small voids for Al-Re alloy-Y2O3 and this is in agreement with the measured porosity 6.84% in this composites.



(a)Al-Re Alloy-Y2O3



(b)Al-Re Alloy-(RHA-Y2O3)[2:2]

Figure 8 SEM Micrographs of (a) Al-Re Alloy-Y2O3 Composite ;(b) Al-Re Alloy-(RHA-Y2O3)[2:2] Hybrid Composite

3.5 X-Ray Diffraction Characterization

Figures 9 show the X-ray diffraction for Al-Re alloy. Three distinct peaks represented by Al, Si, and Al4Ce phases. The major phase is aluminum, while minor phases include Mg2Zn3,AlCe3, AlCuMg, Fe3Si, Al3Ce, La3Al11, Al3Mg and Mg_{102.08}Zn_{39.6}. X-ray pattern for Al-Re alloy shows many small peaks attributed to the reactivity between rare earth elements (Ce and La) and aluminum to form high melting points and infusible compound which dispersed in the alloy. Little literatures available about the effect of addition of rare earth element to Al-alloy (Nieet al., 2002)suggested that the rare earth element can decrease the harm of hydrogen in Al alloys, or act as a modifier , or form high melting points and infusible compound which dispersed in the Al alloy or strengthen the grain boundaries by acting as grain refiners.

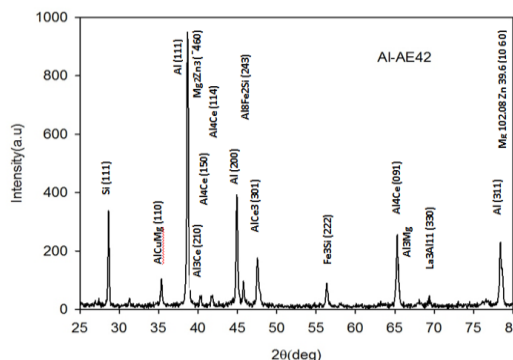


Figure 9 XRD of Al-Re Alloy

The XRD pattern for Al-Re alloy-RHA , Figure 10 shows three distinct peaks represented by Al , Si and SiO2 phases. Two small peaks represented by Al4Ce and Al3Ce. These intermetallic phases are due to the interaction of rare earth with matrix alloy. The β-Mg2SiO4 phase is due to the reaction of silica from RHA with matrix alloy.

The XRD pattern for Al-Re alloy-Y2O3 is shown in Figure 11 with two distinct peaks represented by Al and β -Al2Mg phases. Small minor peaks show in X-ray pattern represented by Al4Ce and YAl phases. The other minor peaks represented by Si and Mg102.08 Zn39.6 phases are belong to the matrix alloy. X-ray pattern for Al-Re alloy-(RHA-Y2O3)[2:2] hybrid composite, Figure 12 shows two distinct peaks represented by Al and Si phases. The major phase is aluminum. Some distinct peaks such as SiO2, C phases are also shown due to the reaction between filler materials and matrix alloy. Al3Ce phase also present due to the interaction between rare earth elements with aluminum matrix. Other minor phases such as Al8Si6Mg3Fe and Fe3Si are belonging to the matrix alloy. In general, peaks result from the addition of filler and rare earth element to the aluminum matrix are small compared with origin matrix phases. The addition of rare earth element in Al-Re alloy-(Y2O3-RHA) hybrid composites lead to the formation of more intermetallic compound between Al and rare earth. This finding is also supported by the work of (Nieet *al.*, (2002).

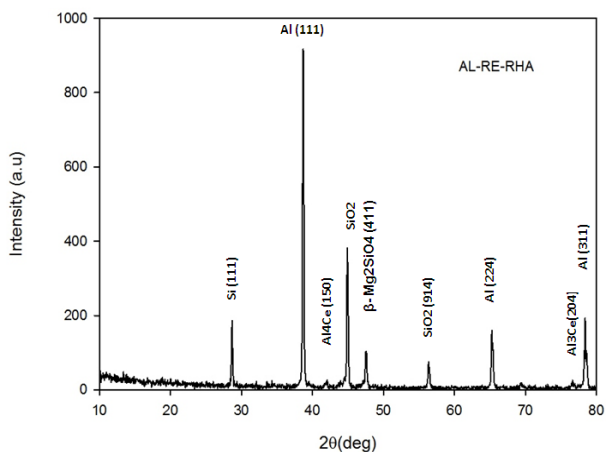


Figure 10 XRD of Al-Re Alloy- RHA Composite

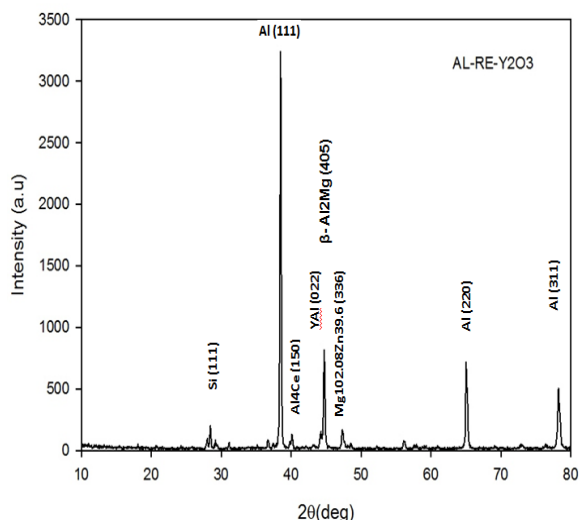


Figure 11 XRD of Al-Re Alloy-Y2O3 Composite

3.6 Hardness of Al-Re Alloy-(RHA-Y2O3) Hybrid Composites

The hardness of the hybrid composites samples was measured by micro-Vickers hardness using 490 gm load for 20second duration time. The hardness test results for Al-Re alloy-(RHA-Y2O3) hybrid composites is shown in Figure 13. The hardness is 52.4 for Al-Re alloy, 63 for Al-Re alloy -RHA composite and 72.3 for Al-Re alloy -Y2O3 composite which is the highest.

The hardness values for Al-Re alloy-(RHA-Y2O3) hybrid composites are between 64.2- 67 for different reinforcement ratio of RHA-Y2O3 and the highest value was 67 at weight ratio of (1:3) of RHA-Y2O3. The hardness of Al-Re alloy - (RHA-Y2O3) hybrid composites increases with increase weight of Y2O3 and the maximum hardness was 72.3 for Al-Re alloy-Y2O3.

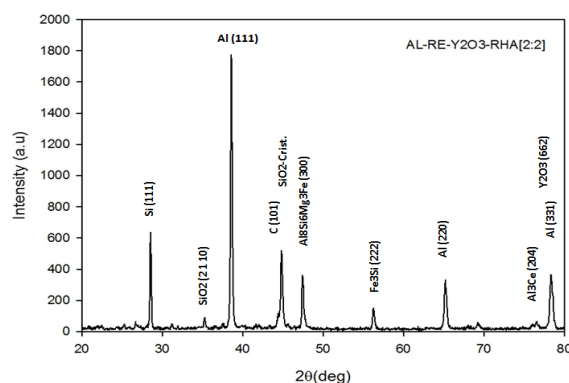


Figure 12 XRD of Al-Re Alloy-(Y2O3-RHA)[2:2] Hybrid Composite

The presence of rare earth elements improve the hardness of Al-Re alloy and Al-Re alloy-(RHA-Y2O3) hybrid composites. The addition of rare earth increase the hardness from 33 for Al-alloy(4032 Al-alloy) to 52.4 for Al-Re alloy due to the following reasons: firstly the formation of intermetallic compound with aluminum such as Al4Ce, Al3Ce, AlCe3 and La3Al11, secondly decrease harm of hydrogen in Al alloy, thirdly grain refinement(Nieet *al.*, 2002).

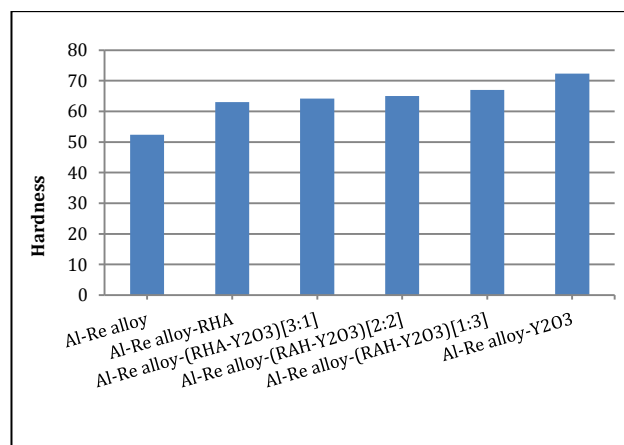


Figure 13 Hardness of Al-Re Alloy and Al-Re Alloy-(RHA-Y2O3) Hybrid Composites

3.7 Apparent Density and Porosity of Al-Re Alloy-(RHA-Y2O3) Hybrid Composites

The measured densities of hybrid composites are shown in Figure 14 and Table5. The measured density is 2.603 gm/cm³ for Al-Re alloy , 2.519 gm/cm³ for Al-Re alloy-RHA composite and 2.697gm/cm³ for Al-Re alloy -Y2O3 composite.

The measured density values for Al-Re alloy-(RHA-Y2O3) hybrid composites are between 2.653 -2.742 gm/cm³ for different reinforcement ratio of RHA-Y2O3 and the highest measured density is 2.742 gm/cm³ at weight ratio of (1:3) of RHA-Y2O3. The measured density of Al-Re alloy-(RHA-Y2O3) hybrid composites increases with increasing wt% of Y2O3. The measured porosity is 2.18% for Al-Re alloy, 3.33 % for Al-Re alloy -RHA composite and the highest porosity is 6.84% for Al-Re alloy -Y2O3 composite. The porosity for Al-Re alloy-(RHA-Y2O3) hybrid composites are between 0.97-3.12 % for different reinforcement ratio.

The measured porosity of Al-Re alloy-(RHA-Y2O3) hybrid composites increases with increasing wt% of Y2O3 as shown in Figure 15. The low porosity is attributed to the use of two-step stirring process that used to producing the composites. The manual mixing process that used in the semi-solid state helps to spread the liquid metal onto the reinforcement particles surface and break the surface gas layers. Surface tension between the aluminum melt and reinforcement particles were reduced to make easier mixing and wetting of particles in the melt (Alaneme and Bodunrin, 2013). The increases in the porosity with increasing of yttrium wt% is due to the agglomeration at higher amount of reinforcement and low wettability in addition to pore nucleation at the Al-alloy matrix/Y2O3 interface (Ezatpouret al., 2013).

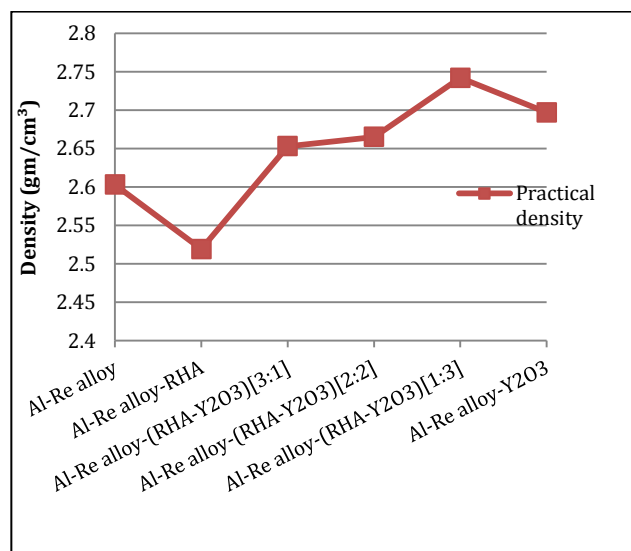


Figure 14 Measured Density of Al-Re Alloy and Al-Re Alloy-(RHA-Y2O3) Hybrid Composites

Table 5 Density and Porosity of Al-Re Alloy and Al-Re Alloy-(RHA-Y2O3) Hybrid Composites

	Composition	Measured Density (gm/cm ³)	Porosity (%)
1	Al-Re Alloy	2.603	2.18
2	Al-Re Alloy-RHA Composite	2.519	3.33
3	Al-Re Alloy-(RHA-Y2O3) [3:1] Hybrid Composite	2.653	0.97
4	Al-Re Alloy-(RHA-Y2O3) [2:2] Hybrid Composite	2.665	3.12
5	Al-Re Alloy-(RHA-Y2O3) [1:3] Hybrid Composite	2.742	2.87
6	Al-Re Alloy-Y2O3 Composite	2.697	6.84

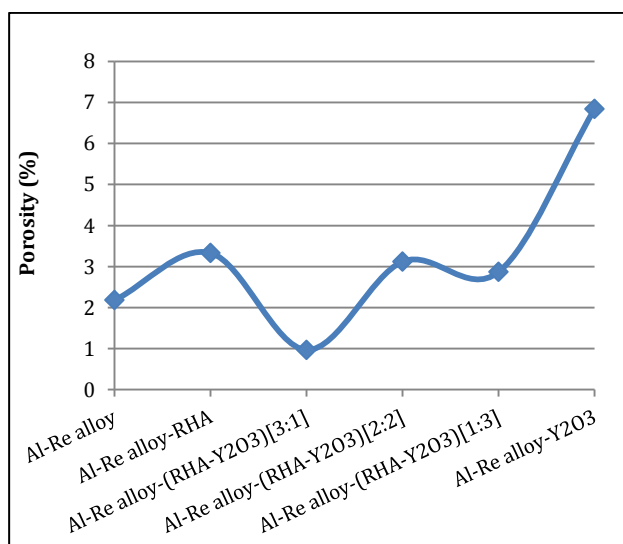


Figure 15 Porosity of Al-Re Alloy and Al-Re Alloy-(RHA-Y2O3) Hybrid Composites

3.8 Wear Behavior

The wear rate results of Al-Re alloy and Al-Re alloy composites revealed that the wear rate increased with increasing the applied load as shown in Figure 16. Both Al-Re alloy-RHA and Al-Re alloy-Y2O3 composites have lower wear rate than Al-Re alloy due to the improvements in the composites hardness caused by the reinforcement. The wear rates of Al-Re alloy-(RHA-Y2O3) hybrid composite is higher than Al-Re alloy at 5N due to the high hardness and abrasion between the asperities of pin surface and the abrasive disk.

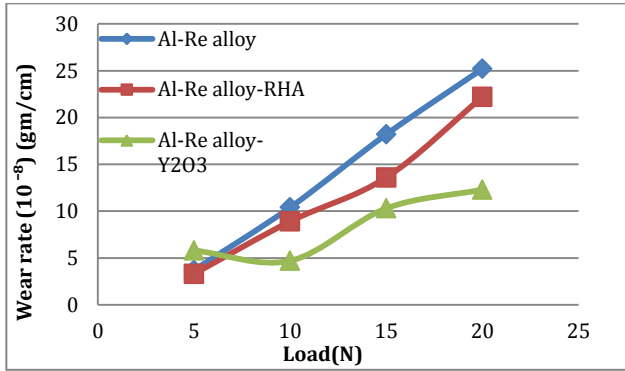


Figure 16 Wear Rate of Al-Re Alloy and Al-Re Alloy-RHA/Y2O3 Composites

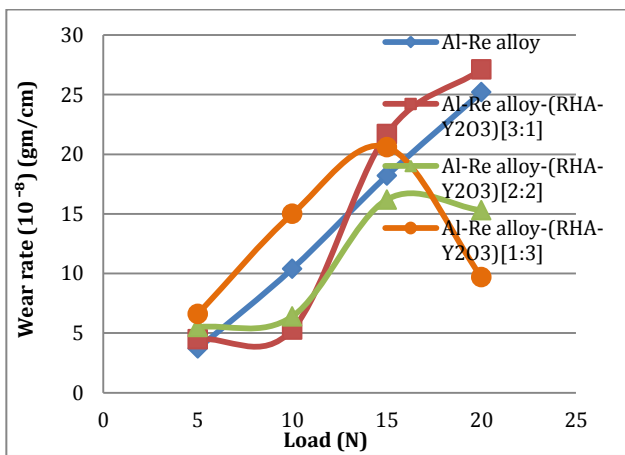


Figure 17 Wear Rate of Al-Re Alloy and Al-Re Alloy-(RHA- Y2O3) Hybrid Composites

For Al-Re alloy-(RHA-Y2O3)[3:1] hybrid composite the wear rate increases very slowly up to 10N and then increases very sharply . This can be attributed to the lubrication property of graphite which increases the wear rate at higher load as shown in Figure 17 . The same finding was observed by (Sharma *et al.*, 2015). Also with increasing the applied load the ability of the penetration of fracture particles (debris) increased and this will increase the removal of material from the sample surface. These fracture particles between disk and sample surface form a three-body system and that increased wear rate (Krishnamurthy *et al.*, 2012) and (Nurani *et al.*, 2015). For Al-Re alloy-(RHA-Y2O3)[1:3] hybrid composite the wear rate increased when the applied load is increased from 5 to 15 N, and then decreased sharply. At load between 5-15N , the fractured asperities leads to higher wear rate. These fracture particles increased and their mean size decreased with increased amount of Y2O3 in hybrid composite. At load 5-15N , this leads to increase the contact area between sliding surfaces and the wear rate is dominated by three-body system. Beyond 15 N ,the wear rate decreased where graphite is squeezed out onto the pin surface due to subsurface deformation and smearing onto the tribosurfaces to produce of lubricant film (Suresh and Kumar, 2013). The

reinforcement particles will be crushed into very small particles and form a very thin surface layer called mechanically mixed layer (MML) which provides protection to the matrix material. The MML layer between the two contact surfaces and provide a protection layer to the matrix material which is very effective in reducing the wear rate (Nurani *et al.*, 2015) . Table 6 shows wear rate for Al-Re alloy and Al-Re alloy composites.

Table 6 Wear Rate of Al-Re Alloy and Al-Re Alloy-(RHA-Y2O3)Hybrid Composites

	Composites	Wear Rate (10 ⁻⁸)(gm/cm)			
		5N	10N	15N	20N
1	Al-Re Alloy	3.7	10.4	18.2	25.2
2	Al-Re Alloy-RHA	3.3	8.9	13.6	22.2
3	Al-Re Alloy-(RHA-Y2O3)[3:1]	4.5	5.3	21.7	27.1
4	Al-Re Alloy-(RHA-Y2O3)[2:2]	5.5	6.4	16.2	15.3
5	Al-Re Alloy-(RHA-Y2O3)[1:3]	6.6	15	20.6	9.7
6	Al-Re Alloy-Y2O3	5.8	4.7	10.3	12.3

Figure 18 shows the variation of wear rate of Al-Re alloy and Al-Re alloy-(RHA-Y2O3)hybrid composites at different loads. In general, the minimum wear rate occurs for Al-Re alloy-Y2O3 composite. At 20N the minimum wear rate occurs at Al-Re alloy-(RHA-Y2O3)[1:3] hybrid composite, while minimum wear rate for 15N and 10N occurs at Al-Re alloy-Y2O3 composite. At 5N, the minimum wear rate occurs at Al-Re alloy-RHA composite.

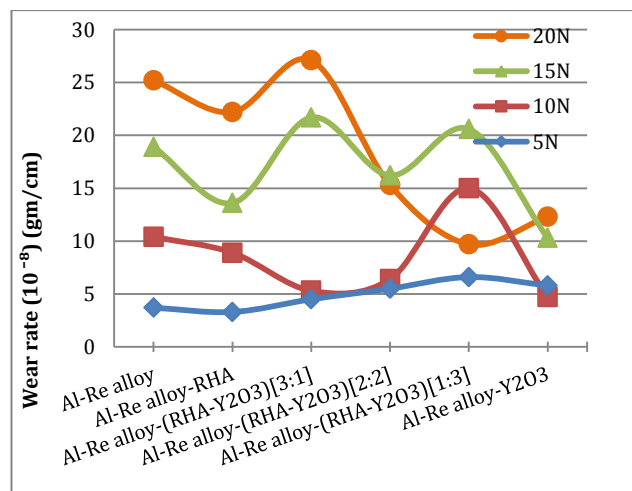


Figure 18 Variation of Wear Rate with different applied loads for Al-Re Alloy-(RHA-Y2O3) Hybrid Composites

3.9 Coefficient of Friction (COF)

The coefficient of friction of unreinforced Al-Re alloy and Al-Re alloy composites were studied at applied loads 5N,10N, 15N and 20N with varying weight percentage of particle reinforcement as shown in Figure 19-20 and Table 7. The maximum coefficient of friction is 0.92 for Al-Re Alloy and for Al-Re Alloy-(RHA-Y2O3)[3:1] Hybrid Composite at 5 N loads as shown in Figure 20. The Al-Re alloy possesses higher coefficient of friction when compared with their composites. This is attributed to uniform mixing of reinforcements with aluminum matrix that result in good bonding between Al matrix alloy and reinforcement particles. These particles act as load bearing members when the applied load increases and this will decrease the contact area between rotating disk and specimen surfaces. Furthermore, the reinforcement particles will restrict the flow of metal during sliding. These reasons lead to decrease the coefficient of friction of composites. This is in agreement with the work of (Singh *et al.*, 2016) who reported that the temperature rise is higher in aluminum matrix alloys when compared with their composites irrespective of surface conditions and applied force. With increase in the applied load, the temperature at specimen interface increases and leads to softening the materials and plastic flow of materials. The Al-Re alloy-RHA composites possess the lowest coefficient of friction at 5N load. This can be attributed to the graphite layer that smeared at the sliding surface and acted as a solid lubricant (Kumar *et al.*, 2014).

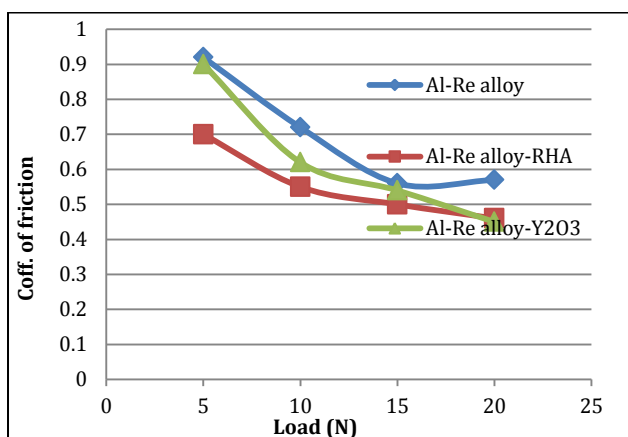


Figure 19 COF of Al-Re Alloy, Al-Re Alloy-RHA Composite and Al-Re Alloy-Y2O3 Composite

Conclusions

Rice husk ash with 91% purity silica was prepared from rice husks by heat treatment at 1100 °C and 2hrs. The hybrid composites Al-Re alloy-(RHA-Y2O3) was prepared using Al-Re alloy and synthetic /Agro waste reinforcement using two steps stir casting. Al-Re alloy hybrid composites have higher hardness value compared with Al-Re alloy. It was found that the

Al-Re alloy-10%Y2O3 composite has lower wear rate for Al-Re alloy hybrid composites. In general, measured density increased with increasing wt% Y2O3 compared with Al-Re alloy, and porosity increased with addition of the reinforcing phase (RHA:Y2O3). The maximum porosity occurs at 10% Y2O3 and minimum value at (RHA-Y2O3)[3:1] hybrid composites. The addition of Y2O3 and the rare earth elements caused refinement in the microstructure of the matrix and the formation of intermetallic compounds.

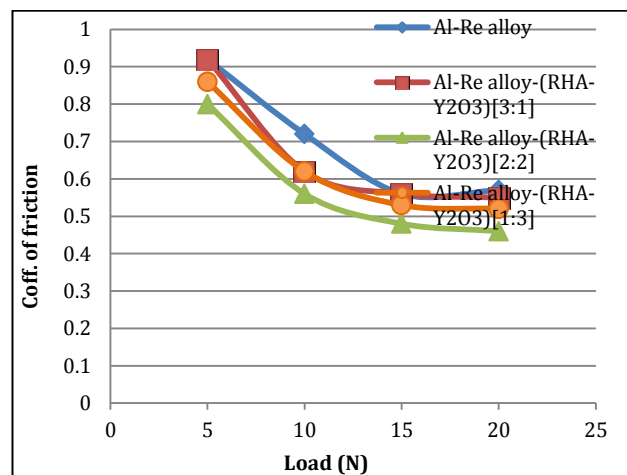


Figure 20 COF of Al-Re Alloy, Al-Re Alloy-(RHA-Y2O3) Hybrid Composite

Table 7 COF of Al-Re Alloy and Al-Re Alloy-(RHA-Y2O3) Hybrid Composites

Composite	COF at 5N	COF at 10N	COF at 15N	COF at 20N
Al-Re Alloy	0.92	0.72	0.56	0.57
Al-Re Alloy- RHA	0.7	0.55	0.5	0.46
Al-Re Alloy-(RHA-Y2O3)[3:1]	0.92	0.62	0.56	0.55
Al-Re Alloy-(RHA-Y2O3)[2:2]	0.8	0.56	0.48	0.46
Al-Re Alloy-(RHA-Y2O3)[1:3]	0.86	0.62	0.53	0.52
Al-Re Alloy-Y2O3	0.9	0.62	0.54	0.45

References

R. Sharma, P. Sharma and G. Singh, (2015) Dry sliding behavior of aluminium alloy reinforced with hybrid ceramic particles, International Journal of Multidisciplinary Research and Development, India, Volume 2(10), pp 485-491.

B. Raju S A, A R K Swamy and A Ramesh, (2014) Mechanical and tribological behavior of aluminum metal matrix composites using powder metallurgy technique- a review, International J. of Mechanical Engineering and Robotics Research, India, Vol. 3(4), pp 551-563.

M.A. Maleque, A. Atiqah, R.J. Talib, H. Zahurin, (2012) Journal of Mechanical and Materials Engineering, 7(2) p.166.

P. B. Madakson, D. S. Yawas, A. Apasi (2012). International Journal of Engineering Science and Technology (IJEST) 4 (3): 1190-1198.

- A. M. Usman, A Raji and N. H. Waziri, (2014) Characterisation of Girei Rice Husk Ash for Silica Potential, journal of environmental science, toxicology and food technology, Nigeria, Vol. 8 (1), PP 68-71.
- C. Saravanan, K. Subramanian, V. A. Krishnan and R. S. Narayanan, (2015) Effect of Particulate Reinforced Aluminum Metal Matrix Composite -A Review, Mechanics and Mechanical Engineering, Lodz University of Technology, Vol.19(1), pp 23-30.
- S. Mathur and A. Barnawal, (2013) Effect of Process Parameter of Stir Casting on Metal Matrix Composites, International Journal of Science and Research, India, Vol. 2 (12), pp 395-397.
- K.T Shridhara, S.Hanumthall and A.Rao(2015), Characterization of aluminum-copper alloy with bamboo leaf ash and graphite metal matrix composites, international journal of engineering, Vol.4(7), pp 446-450.
- D. S. Prasad, Ch. Shoba and N. Ramanaiah, (2014) Investigation on mechanical properties of aluminum hybrid composites, journal of material research and technology, Vol. 3(1), pp 79-85.
- A. M. Usman, A.Raji, N. H. Waziri and M. A. Hassan, (2014) Aluminum alloy - rice husk ash composites production and analysis, leonardo electronic journal of practices and technologies, Vol. Issue, pp 84-98.
- D. S. Prasad and Ch. Shoba, (2014) Hybrid composites-a better choice for high wear resistant materials, journal of material research and technology, Vol. 3(2), pp 172-178.
- K.K. Alaneme and T.M. Adewale, (2013) Influence of rice husk ash - silicon carbide weight ratios on the mechanical behavior of Al-Mg-Si alloy matrix hybrid composites, tribology in industry, Vol. 35(2), pp 163-172.
- S.D. Saravanan and M.S. Kumar, (2013) Effect of Mechanical Properties on Rice Husk Ash Reinforced Aluminum alloy (AlSi10Mg) Matrix Composites, International Conference on Design and Manufacturing, IConDM 2013, Procedia Engineering, Vol. 64, 1505-1513.
- A. Mittal and R. Muni, (2013) Fabrication and characterization of mechanical properties of Al-RHA-Cu hybrid metal matrix composites, International journal of current engineering and technology, Vol. 3(5).
- K. k. Alaneme and P. A. Olubambi, (2013) Corrosion and wear behavior of rice husk ash-alumina reinforced Al-Mg-Si alloy matrix hybrid composites, journal of material research and technology, Vol. 2(2), pp188-194.
- H. P. Pydi, H K R Prasad Saripalli, M. R. Abburi, B.S.B. Murthy and D.Sivaprasad, (2012) Scanning electron microscope studies on dry sliding wear behavior of metal matrix composites with aluminum and rice husk ash, international journal of integrative sciences, Innovatn and technology, Vol. 1(2), pp1-5.
- H. R. Saleh, (2012) Mechanical properties of the modified Al-12%Si alloy reinforced by ceramic particles, Engineering and technology journal, Vol. 28(2).
- W.B. Bouaeshi and D.Y. Li, (2007) Effects of Y2O3 addition on microstructure, mechanical properties, electrochemical behavior, and resistance to corrosive wear of aluminum, Tribology International, Vol. 40, pp 188-199.
- ASM handbook, Nonferrous Alloys and Special-Purpose Materials, Vol. 2, 1992.
- A.Moosa, A.Y.Awad, (2016) Influence of Rice Husk Ash-Yttrium Oxide Addition on the Mechanical Properties Behavior of Aluminum Alloy Matrix Hybrid Composites, International Journal of Current Engineering and Technology, Vol.6, No.3.
- ASM Handbook, Mechanical Testing and Evaluation, Vol. 8, 2000.
- N. Prasad, H. Sutar, S. Ch. Mishra, S. K. Sahoo and S. K. Acharya, (2013) Dry Sliding Wear Behavior of Aluminum Matrix Composite Using Red Mud an Industrial Waste, International Research Journal of Pure & Applied Chemistry, Vol.3(1), PP 59-74.
- M. Boopathi, K.P. Arulshri and N. Iyandurai, (2013) Evaluation of mechanical properties of aluminum alloy 2024 reinforced with silicon carbide and fly ash hybrid metal matrix, American journal of applied sciences, Vol. 10(3), pp 219-229.
- J. Hashim, L. Looney and M.S.J. Hashmi, (1999) Metal matrix composites: production by the stir casting method, Journal of Materials Processing Technology, Ireland, Vol.92 (93), pp 1-7.
- K. K. Alaneme, (2013) Mechanical Behavior of Cold Deformed and Solution Heat-treated Alumina Reinforced AA 6063 Metal Matrix Composites, The West Indian Journal of Engineering, Vol. 35(2), pp 31-35.
- K.K. Alaneme, Y.O. Anabaranze and S.R. Oke, (2015) Softening Resistance, Dimensional Stability and Corrosion Behavior of Alumina and Rice Husk Ash Reinforced Aluminum Matrix Composites Subjected to Thermal Cycling, Tribology in Industry, Vol. 37(2), pp 204-214.
- A. A. Ramezani-pour, M. M. khani and Gh. Ahmadibeni, (2009) The Effect of Rice Husk Ash on Mechanical Properties and Durability of Sustainable Concretes, International Journal of Civil Engineering. Vol. 7(2), pp 83-91.
- A.D. Onojah, N.A. Agbendeh and C. Mbakaan, (2013) Rice husk ash refractory: The temperature dependent crystalline phase aspects, IJRRAS, Vol. 15(2), pp 246-248.
- K. Nogita, S. D. McDonald and A. K. Dahle, (2004) Eutectic Modification of Al-Si Alloys with Rare earth Metals, Materials Transactions, Japan Institute of Metals, Vol. 45(2), pp 323-326.
- A. S. Anasyida, A. R. Daud and M. J. Ghazali, (2010) Dry sliding wear behavior of Al-12Si-4Mg alloy with cerium addition, Materials and Design, Vol. 31, pp 365-374.
- Z. Nie, T. Jin, Jingbou FU, Guefu XU, J. YANG, J. ZHOU and T.Zuo, (2002) Research on Rare earth in Aluminum, Materials Science Forum, Vol. 396(402), pp 1731-1736.
- K. K. Alaneme and M. O. Bodunrin, (2013) Mechanical behavior of Aluminum reinforced AA 6063 metal matrix composites developed by two step-stir casting process, Acta Technica Convinesis- Bulletin of Engineering, pp 105-110.
- H. R. Ezatpour, M. Torabi -Parizi and S. A. Sajjadi, (2013) Microstructure and mechanical properties of extruded Al/Al2O3 composites fabricated by stir-casting process, Transactions of Nonferrous Metals Society of China, Vol. 23, pp 1262-1268.
- D. S. Prasad and A. R. Krishna, (2012) Tribological Properties of A356.2/RHA Composites, Journal of Material Science and Technology, Vol. 28(4), pp 367-372.
- N. Krishnamurthy, M. S. Prashanthareddy, H. P. Raju, and H. S. Manohar, (2012) A Study of Parameters Affecting Wear Resistance of Alumina and Yttria Stabilized Zirconia Composite Coatings on Al-6061 Substrate, International Scholarly Research Network, pp 1-13, Vol. 2012.
- Sh. J. Nurani, Ch. K. Saha, and M. N Haque, (2015) Mechanical Properties and Wear Strengths of Piston Alloy-Alumina Composites, International Journal of Innovative Science and Modern Engineering, Vol. 3(2), pp 75-79.
- R. Suresh and M. P. Kumar, (2013) Investigation of Tribological behavior and its Relation with Processing and Microstructures of Al 6061 Metal Matrix Composites, International Journal of Research in Engineering & Technology, Vol. 1(2), pp 91-104.
- K. K. Singh, S. Singh and A. K. Shrivastava, (2016) Study on tribological behavior of silicon carbide based aluminum metal matrix composites under Dry and Lubricated environment, To be published in J. of Advances in Materials Science and Engineering.
- S.J. Kumar, G. Santhosh, D. Nirmalkumar, A. Saravanakumar, P. Sasikumar and S. Sivasankaran, (2014) Mechanical and Dry Sliding Wear Behavior of Al6063/ Al2O3/ Graphite Hybrid Composites, International Journal of Innovative Research in Science, Engineering and Technology, Vol. 3(3), pp 1222-1228.